Toward the LES of flow past a submerged hydrofoil

By A. Pascarelli †, G. Iaccarino AND M. Fatica

The fluid flow past a body placed in a steady stream close to a free surface is the object of the current investigation. The viscous, incompressible Navier-Stokes equations, supplemented by linearized dynamic and kinematic boundary conditions at the free surface, are solved so that the water-surface elevation can be integrated into the solution and solved for, together with the velocity and pressure fields. The potential and limitations of the method will be illustrated and discussed.

1. Introduction

Incompressible viscous fluid flows bounded by a free surface have a number of interesting properties. The free-surface boundary is in motion, its location is part of the solution, and the relative velocity between the fluid and surface interface must vanish. In addition, the tangential stress at the surface must vanish, and the normal stress must balance the ambient pressure above the surface. As a result, when a vortex interacts with a free surface, the velocity field is significantly altered and this results in a complex structure and dynamics. For a free surface without contamination or external shear stress (idealized free surface), the vorticity at the free surface depends on the shape of the boundary (and on the assumed boundary conditions). If the free surface can be considered flat (i.e., of negligible deformation) the vortical field close to the interface is very similar to that near a free-slip plane. For a shear-free interface in which no deformations are allowed, the tangential vorticity (and its fluctuations), but not necessarily the flux of vorticity, vanishes at the free surface. The boundary condition of zero shear stress at a clean free surface requires that vortex lines which terminate at the free surface be normal to the surface. In the case of a shear-free deformed free surface, however, the vorticity at the free surface is nonzero and the surface acquires a solid body rotation due to the boundary condition allowing motion parallel to the surface. For example, in the interaction of a vortex pair with a free surface (see figure 1), the surface renewal produced by vortices with vorticity parallel to the surface already shows that the surface deformation will be an important feature of the turbulent transport at the interface. The aim of this work is to investigate the characteristics of the complex viscous interaction of the free surface with the wake of an isolated lifting hydrofoil submerged at relatively shallow depth, for moderate Froude numbers. This investigation is a precursor to a turbulent flow study at $Re = 30,000$, planned as a follow-up.

† INSEAN - Roma, ITALY

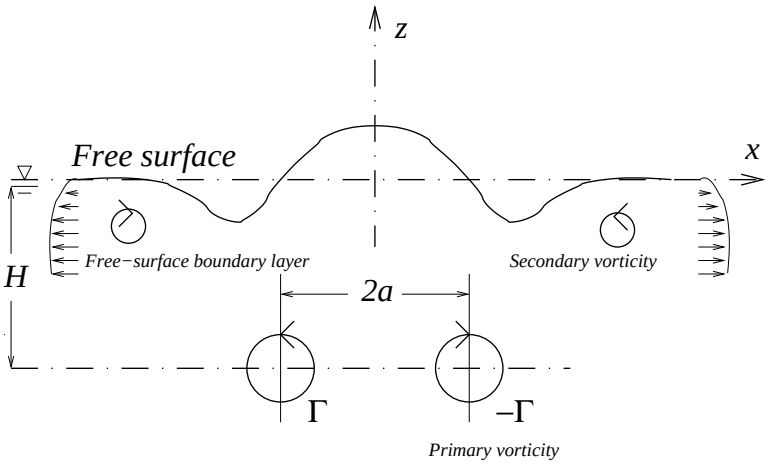

FIGURE 1. Sketch of a vortex pair impinging on a free surface.

2. Mathematical model

2.1. *Governing equations*

In Cartesian coordinates x_i $(i = 1, 2, 3) \equiv (x, y, z)$ the governing equations for an incompressible viscous flow, in the presence of body forces, of a layer of fluid of uniform depth H can be written in the following form

$$\frac{\partial u_j}{\partial x_j} = 0\,, \quad \frac{\partial u_i}{\partial t} + \frac{\partial}{\partial x_j}\left(u_j u_i\right) = -\frac{1}{\rho}\frac{\partial p}{\partial x_i} + \frac{1}{\rho}\frac{\partial \sigma_{ji}}{\partial x_j} + f_i \tag{2.1}$$

where the summation convention applies to repeated indices. Here, ρ and $\nu = \mu/\rho$ are the (constant) fluid density and kinematic viscosity respectively, t is the time, and u_i $(i = 1, 2, 3) \equiv (u, v, w)$ are the Cartesian fluid-velocity components. The vertical coordinate $z \equiv x_3$ is positive measured upwards from the flat, horizontal solid bottom surface, $z = H$ coincides with the undisturbed free surface level, while $z = 0$ corresponds to the position of the solid bottom. Let $F(x, y, z, t) = 0$ be the free-surface equation. Assuming no wave overturning or breaking, $F = F(x, y, z, t)$ is a single-valued function of x and y and can be expressed as

$$F(x, y, z, t) = \eta(x, y, t) - (z - H) = 0 \tag{2.2}$$

where η is the displacement of the free surface about the horizontal plane $z = H$. Relating the modified, or hydrodynamic, pressure p to the pressure P by $p = P + \rho g \eta$, g being the acceleration due to gravity, gravity effects appear only in the dynamic free-surface boundary condition. Like P, p appears in the equations through its gradient and is thus defined to within an arbitrary constant which is fixed by boundary conditions. The nonlinear advection term is written in conservation form. The viscous stress tensor σ_{ji} is expressed as a function of the strain-rate tensor $S_{ij} = (\partial u_i/\partial x_j + \partial u_j/\partial x_i)/2$, according to $\sigma_{ij} = 2\mu S_{ij}$. The source term f_i represents a body force per unit mass, arising from the immersed-boundary technique described below, which may vary as a function of time and space.

In flow problems involving free surfaces, part of the boundary of the computational domain (corresponding to the free surface) is unknown, and must be determined as part of the solution. On the free surface, two boundary conditions should be satisfied. The first boundary condition is determined from the balance of the stresses acting on the

interface between the upper and lower fluid layers, in the normal and tangential directions (so-called "dynamic" boundary condition). The specification of this force balance must depend on the nature of the particular physical situation being modelled. In this study, the free surface is considered as an uncontaminated free boundary between two immiscible fluids (water and air) on which no tangential stresses are imposed on its air-side. Moreover, given the water/air density ratio $\rho/\rho_a \approx 820$, we further assume the upper fluid layer light enough to cause no significant variation in hydrostatic or dynamic pressure, and both density and viscosity of the air phase are set to zero (vacuum approximation). For dynamic boundary conditions at a liquid-gas interface, with negligible viscous stresses in the gas and gradient of surface tension, we have, in general,

$$-P + \sigma_n = -P_a + \sigma_s k_s\,, \quad \sigma_t^{(l)} = 0 \quad l = 1, 2 \tag{2.3}$$

Here P_a denotes the external pressure, which we set to an arbitrary constant, say $P_a = 0$. σ_s is the (constant) surface tension coefficient (in units of force per unit length), k_s is the local interfacial curvature. $\sigma_n = n_i \sigma_{ji} n_j$ and $\sigma_t^{(l)} = t_i^{(l)} \sigma_{ji} n_j$, $l = 1, 2$ are the normal and the two tangential components of the viscous stress vector at the interface, in which n_i, $t_i^{(l)}$ are the $i-$direction components of unit vectors, the outward normal to the free surface and the two tangential to the free surface in the $(x, z)-$ and $(y, z)-$planes, respectively.

The second boundary condition at the free surface (called "kinematic") is formulated by considering that a fluid particle on the free surface remains on it, i.e. $\mathbf{u} \cdot \mathbf{n} = -(\partial F/\partial t)/|\nabla F|$ where everything is evaluated at the exact position of the free surface, $F(x, y, z, t) = 0$, and $|\nabla F| = \left[(\partial F/\partial x_i)^2\right]^{1/2}$. For a free surface given by (2.2) we have $\mathbf{n}(x, y, z) \equiv [-\eta_x, -\eta_y, 1] \left(\eta_x^2 + \eta_y^2 + 1\right)^{-1/2}$, $\mathbf{t}^x(x, y, z) \equiv [1, 0, \eta_x] \left(\eta_x^2 + 1\right)^{-1/2}$, $\mathbf{t}^y(x, y, z) \equiv [0, 1, \eta_y] \left(\eta_y^2 + 1\right)^{-1/2}$, and

$$k_s = \frac{\eta_{xx}(1 + \eta_y^2) - 2\eta_x \eta_y \eta_{xy} + \eta_{yy}(1 + \eta_x^2)}{\left(1 + \eta_x^2 + \eta_y^2\right)^{3/2}}.$$

Therefore, executing the dot product $\mathbf{u} \cdot \mathbf{n}$ the above condition can be rewritten as

$$w = \eta_t + u\eta_x + v\eta_y \quad \text{on} \quad z = \eta + H \tag{2.4}$$

Equation (2.4) represents a non-linear boundary condition; the wave elevation η is an unknown function of time and space and must be determined as part of the solution. The dynamic boundary conditions are written as

$$p = \rho g \eta + 2\rho\nu \frac{\left[w_z - (u_z + w_x)\,\eta_x - (v_z + w_y)\,\eta_y + u_x \eta_x^2 + (v_x + u_y)\,\eta_x \eta_y + v_y \eta_y^2\right]}{\left(\eta_x^2 + \eta_y^2 + 1\right)} - \sigma_s k_s \tag{2.5}$$

for the normal direction and

$$\left(1 - \eta_x^2\right)(u_z + w_x) + 2\eta_x\,(w_z - u_x) - \eta_y\,(u_y + v_x) - \eta_x \eta_y\,(v_z + w_y) = 0 \tag{2.6}$$

$$\left(1 - \eta_y^2\right)(v_z + w_y) + 2\eta_y\,(w_z - v_y) - \eta_x\,(u_y + v_x) - \eta_x \eta_y\,(u_z + w_x) = 0 \tag{2.7}$$

for the tangential directions. Again, note that each term is evaluated on the interface, $z = \eta + H$. Neglecting effects of nonlinear self-interactions of surface waves, we assume that the wave elevation in the physical region is small ($|\eta| << 1$), and the interfacial boundary conditions are linearized by assuming a free-surface deformation of order $\epsilon \sim O(Fr^2)$ and a free-surface boundary layer of thickness $\delta \sim O(Re^{-1/2})$, with $\delta^2 \ll \epsilon \ll \delta \ll 1$: see Tsai

& Yue (1995). Upon Taylor expansion about $z = H$ and using continuity we obtain the kinematic boundary condition to be enforced at the undisturbed free surface,

$$w = \eta_t + (u\eta)_x + (v\eta)_y \quad \text{on} \quad z = H. \tag{2.8}$$

Finally, for small slopes $\mathbf{n} \simeq [-\eta_x, -\eta_y, 1]$, $\mathbf{t}^{(1)} \simeq [1, 0, \eta_x]$, $\mathbf{t}^{(2)} \simeq [0, 1, \eta_y]$, and $k_s \simeq \eta_{xx} + \eta_{yy}$, so that the balance of the normal and the two tangential stress components at the unperturbed interface $z = H$ may be described conveniently by

$$p = \rho g \eta + 2\rho\nu w_z - \sigma_s \left(\eta_{xx} + \eta_{yy}\right) \text{ on } z = H \tag{2.9}$$

$$(u_z + w_x) = 0 \text{ on } z = H \tag{2.10}$$

$$(v_z + w_y) = 0 \text{ on } z = H \tag{2.11}$$

Conditions (2.9)–(2.10)–(2.11) allow a velocity across the boundary.

Usually, all the variables are made dimensionaless by a characteristic flow velocity u_{ref} and a characteristic length scale l_{ref}. The case-specific nondimensional groups in these flows are the Reynolds number, the Froude number and the Weber number. The relevant nondimensional parameter is the Reynolds number, defined as $Re = u_{ref} l_{ref}/\nu$, whereas the effect of the free-surface boundary condition is expressed in terms of the dimensionless Froude number, $Fr = u_{ref}/\sqrt{g l_{ref}}$, and Weber number, $We = \rho l_{ref} u_{ref}^2/\sigma_s$, which will appear in the condition (2.9). The Froude number is (the square root of) the ratio of inertia to gravity (or buoyancy), and, since it compares a given characteristic flow velocity to that of (long-wavelength) gravity waves, it directly relates to the speed of a surface disturbance. The Weber number represents surface-tension effects on the free surface. Capillary effects are negligible when the Weber number is large. The case of a free-slip plane surface corresponds to the limit $Fr = 0$ of the present problem. In such a flow, in which the gravity g is infinite, inviscid no-stress boundary conditions (i.e, $u_z = v_z = w = 0$, and $p_z = 0$) are imposed at the interface corresponding to the "free surface", and the physical phenomena observed there will be expected to be independent of groups such as the Froude and Weber numbers. The boundary conditions at the free surface influence quantities that involve derivatives of the velocity, which for example has interesting consequences for the vorticity at the free surface. It is of interest to note that while tangential vorticity at a flat free surface is always zero, the zero-stress boundary conditions (2.10)–(2.11) yield surface vorticity components

$$\omega_x = w_y - v_z = -2v_z = 2w_y \quad \text{on} \quad z = H \tag{2.12}$$

$$\omega_y = u_z - w_x = 2u_z = -2w_x \quad \text{on} \quad z = H. \tag{2.13}$$

2.2. *Discretization method*

The governing equations, supplemented by linearized dynamic and kinematic boundary conditions at the free surface, are solved by a fractional-step/finite-difference algorithm based on a staggered-grid formulation (Chorin 1967, Kim & Moin 1985). The overall accuracy of the method is second order in time and space. It is close to the method presented in Shen *et al.* (1999); however the equation of energy conservation has been explicitly taken into account in the numerical discretization. An immersed-boundary technique is used to handle the presence of the solid body in the fluid stream. The "direct forcing method" proposed by Fadlun *et al.* (2000) has been implemented. The discussion here is purposely kept brief because a complete description can be found in Pascarelli *et al.* (2002) and Fadlun *et al.* (2000).

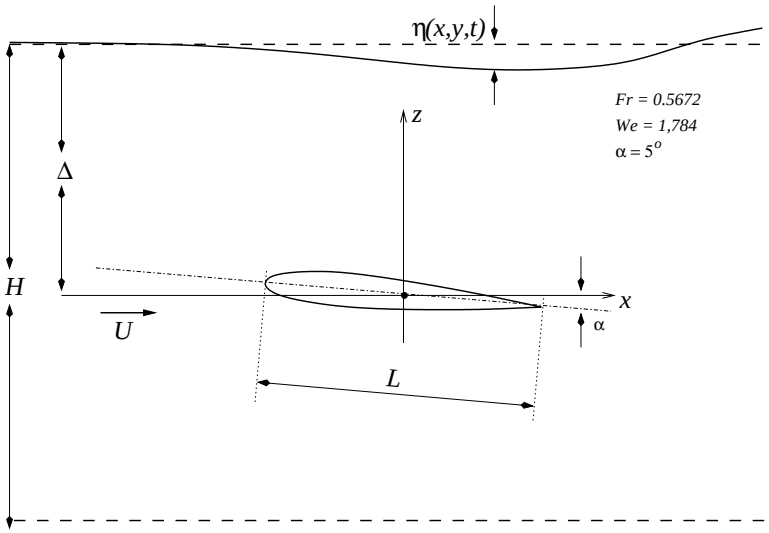

FIGURE 2. Geometry of the flow past a submerged hydrofoil.

3. Results

3.1. *Flow over a submerged hydrofoil*

We consider the flow of water around an hydrofoil which is below a free surface. The hydrofoil section considered is NACA 0012 with an angle of attack of 5^o. The arrangement consists of a two-dimensional open channel whose upper boundary is a free surface. In this system, quantities are nondimenzionalized with the chord length of the body ($l_{ref} = L$) and the uniform inflow velocity ($u_{ref} = U_{in}$). Based on these scales the relevant non-dimensional parameters include the Reynolds number $Re = U_{in}L/\nu$, the Froude number $Fr = U_{in}/\sqrt{gL}$, and the Weber number $We = \rho L U_{in}^2/\sigma_s$. Other geometric parameters in this problem are the upstream length L_u and the downstream length L_d. This problem reproduces the case studied experimentally (Duncan (1983)) and modelled numerically by several authors (Hino, Martinelli & Jameson (1989), Muscari & Di Mascio (2002)) at $Re = 1.624 \times 10^5$, $Fr = 0.5672$ and $We = 1784$. At any fixed dimensionless depth of submergence $\gamma = \Delta/L$, the wave amplitude (and hence wave resistance) possesses a maximum as a function of Froude number based on submergence depth $Fr_\Delta = U_{in}/(g\Delta)^{1/2}$. When that maximum is sufficiently low, linearization is justified. In our simulations the body centre is submerged at mid-chord by $\gamma = 1.034$. At this submergence the leading wave does not break. For our purposes, it is convenient to consider the situation from a frame of reference that is at rest with the body. The domain is 18.5 units in length (the upstream boundary is 6 units upstream of ht eleading edge) and 4 units in depth. In order to prevent any reflection of waves into the solution domain, an artificial damping function for η is used at the downstream boundary. The damping length is set to $l_d = 2L$. Non-uniform mesh distributions are used in both x- and z-directions, with grid clustering near the body surface. With the same Froude and Weber numbers, this flow was investigated in the Reynolds number range from 500 to 10000, far lower than the reference experimental data, but only results for the most interesting cases are reported here. Figure 3 shows the wave profiles for different Reynolds numbers. Viscous effects significantly affect the wave amplitude. Unfortunately, no experimental date are available for low Reynolds number to compare with the results. For the 2D simulations, a total of

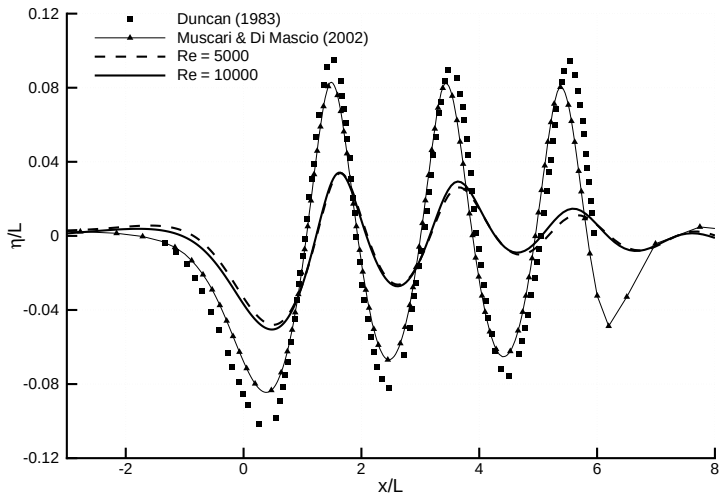

FIGURE 3. Submerged NACA 0012. Wave profiles for different Reynolds numbers.

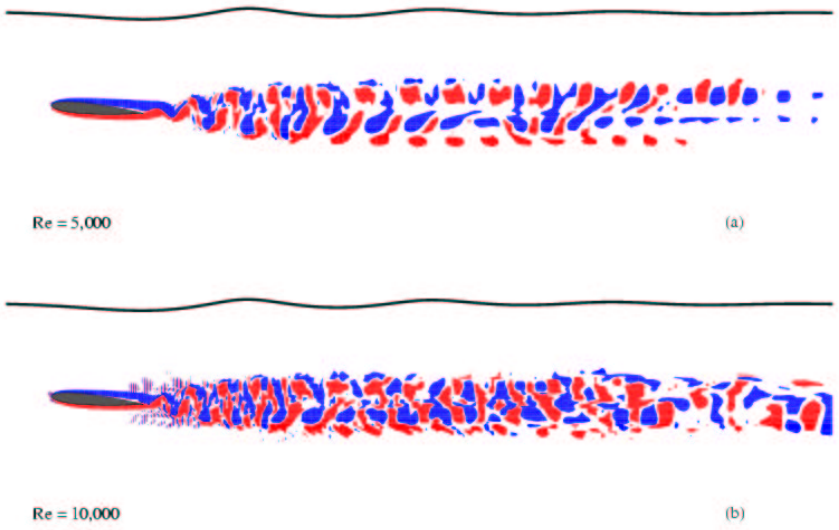

FIGURE 4. Vorticity contours for flow over submerged NACA 0012 at $t = 45$: (a) $Re_b = 5000$; (b) $Re_b = 10000$. Only part of the domain is shown.

$nx = 780$ computational cells are used in the x-direction, while the total number of cells in the vertical direction is $nz = 200$. 4246 grid points are placed within the body. As also observed by Chen & Chwang (2002) as the Reynolds number is increased up to 5000 the von Karman street converges to an oscillatory motion. For $Re = 10000$, the flow reaches a transitional stage and transition is about to occur. The instantaneous vorticity contours for $Re = 5000$ and $Re = 10000$ are shown in figure 4 (a) and in figure 4 (b), respectively. Finally, the force coefficients for the two Reynolds numbers are plotted in figure 5. It is clear from figure 4 (b) that, despite the dense grid clustering around the body, which also

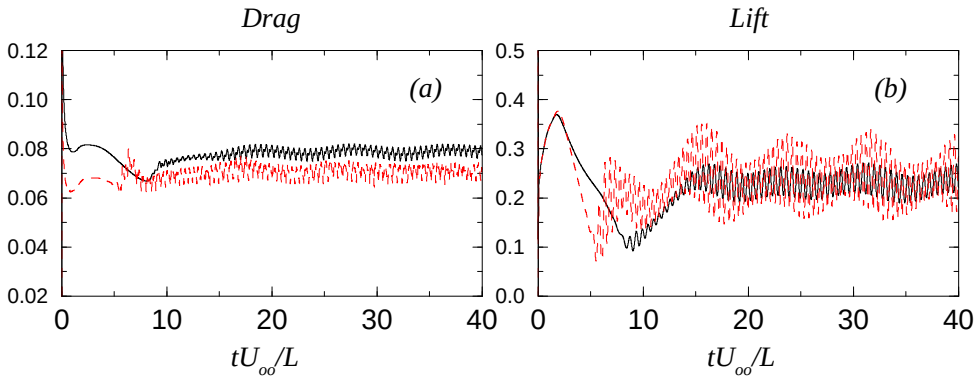

FIGURE 5. Variation of force coefficients during early wake formation with time from an impulsive start. (*a*) Drag coefficient and (*b*) lift coefficient: ——— $Re = 5000$; - - - $Re = 10000$.

restricts the computational time step, the mesh resolution is not sufficient even at the moderate Reynolds number $Re = 10000$ and spurious numerical oscillations are detected. The absence of any artificial control (numerical dissipation) of the odd-even decoupling in the solution results in a serious issue when an advection equation for the free surface is solved along with the flow field. The occurence of wiggles in the velocity field at time t^n may affect the solution quality at the vnext time step through the Dirichlet boundary condition on the pressure field. We found that lack of resolution can result in numerical oscillations that can obscure the flow field.

3.2. *Flow around a free-surface-piercing square cylinder*

As an example of further applications of the present simulation technique the free–surface flow resulting from a partially-submerged square cylinder is considered.

The study of this flow is extremely complicated because of the strong interaction between the free surface and the solid object; in the previous case, only the effect of the presence of the submerged body (via the pressure and eventually the vorticity) was felt on the free surface.

The immersed-boundary technique employed here provides a very natural framework to treat problems involving partially-submerged bodies. Using the same assumptions as previously, only the part of the fluid up to the free-surace is considered. The solid body is represented through a "direct" forcing on the velocity field (in the momentum equations) whereas the pressure field is obtained solving the unmodified elliptic equation arising from the fractional-step procedure. The same treatment is applied to the kinematic boundary condition on the free surface, which accounts for the presence of the cylinder directly through the velocity field in 2.9.

Only proof-of-concept simulations have been carried out so far; a low Reynolds number ($Re = 500$) is considered and the free surface elevation is shown in figure 6.

Further analysis will be required to verify the accuracy of the present linearized free-surface boundary conditions in the presence of surface-piercing bodies.

Acknowledgments

A.P. would like to thank Dr. A. Di Mascio for his input in many useful discussions.

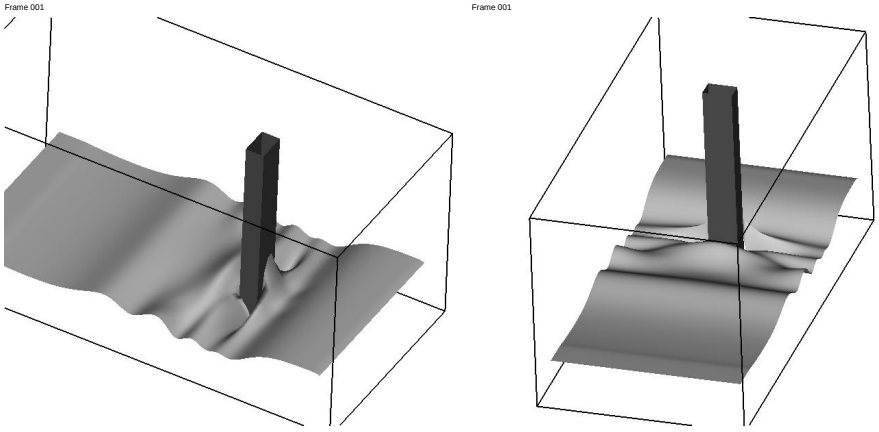

FIGURE 6. Wave elevation for a surface-piercing square cylinder: (*a*) Side View; (*b*) View from behind.

REFERENCES

CHEN, T. & CHWANG, T. 2002 Trailing vortices in a free-surface flow. *Phys. Fluids* **14**, 827–838.

CHORIN, A. J. 1967 A numerical method for solving incompressible viscous flow problems. *J. Comput. Phys.* **2**, 12–26.

DUNCAN, J. H. 1983 The breaking and non-breaking wave resistance of a two-dimensional hydrofoil. *J. Fluid Mech.* **126**, 507–520.

FADLUN, E. A., VERZICCO, R., ORLANDI, P. AND MOHD-YUSOF, J. 2000 Combined immersed-boundary finite-difference methods for three-dimensional complex flow simulations. *J. Comput. Phys.* **161**, 35–60.

HINO, T., MARTINELLI, L. & JAMESON, A. 1993 A finite volume method with unstructured grid for free-surface flow. *Proc. 6th International Conference on Num. Ship Hydrodynamics, Iowa City, IA*, 173–194.

KIM, J. & MOIN, P. 1985 Application of a fractional-step method to incompressible Navier-Stokes equations. *J. Comput. Phys.* **59**, 308–323.

MUSCARI, R. & DI MASCIO, A. 2002 A model for the simulation of spilling breaking waves. To appear in J. Ship Research

ORLANSKI, I. 1976 A simple boundary condition for unbounded hyperbolic flows. *J. Comput. Phys.* **21**, 251–269

PASCARELLI, A., BROGLIA R. & DI MASCIO, A. 2002 Numerical simulations of laminar free-surface flows. In preparation.

SHEN, L., ZHANG, X., YUE, D. K. & TRIANTAFYLLOU, G. S. 1999 The surface layer for free-surface turbulent flows. *J. Fluid Mech.* **386**, 167–212.

TSAI, W.-T. & YUE, D. K. P. 1995 Effects of soluble and insoluble surfactant on laminar interaction of vortical flows with a free surface. *J. Fluid Mech.* **289**, 315–349.